Pharmacologic targeting of the p62 ZZ domain enhances both anti-tumor and bone-anabolic effects of bortezomib in multiple myeloma

Silvia Marino,[1] Daniela N. Petrusca,[1] Ryan T. Bishop,[2] Judith L. Anderson,[1] Hayley M. Sabol,[3] Cody Ashby,[4] Justin H. Layer,[1] Annamaria Cesarano,[1] Utpal P. Davé,[1] Fabiana Perna,[1] Jesus Delgado-Calle,[3,5] John M. Chirgwin[1,6] and G. David Roodman[1,6]

[1]Department of Medicine, Division of Hematology/Oncology, Indiana University School of Medicine, Indianapolis, IN; [2]Department of Tumor Biology, H. Lee Moffitt Cancer Research Center and Institute, Tampa, FL; [3]Department of Physiology and Cell Biology, University of Arkansas for Medical Sciences, Little Rock, AR; [4]Department of Biomedical Informatics, University of Arkansas for Medical Sciences, Little Rock, AR; [5]Winthrop P. Rockefeller Cancer Institute, University of Arkansas for Medical Sciences, Little Rock, AR and [6]Research Service, Roudebush Veterans Administration Medical Center, Indianapolis, IN, USA

Abstract

Multiple myeloma (MM) is a malignancy of plasma cells whose antibody secretion creates proteotoxic stress relieved by the N-end rule pathway, a proteolytic system that degrades N-arginylated proteins in the proteasome. When the proteasome is inhibited, protein cargo is alternatively targeted for autophagic degradation by binding to the ZZ-domain of p62/sequestosome-1. Here, we demonstrate that XRK3F2, a selective ligand for the ZZ-domain, dramatically improved two major responses to the proteasome inhibitor bortezomib (Btz) by increasing: i) killing of human MM cells by stimulating both Btz-mediated apoptosis and necroptosis, a process regulated by p62; and ii) preservation of bone mass by stimulating osteoblast differentiation and inhibiting osteoclastic bone destruction. Co-administration of Btz and XRK3F2 inhibited both branches of the bimodal N-end rule pathway exhibited synergistic anti-MM effects on MM cell lines and CD138+ cells from MM patients, and prevented stromal-mediated MM cell survival. In mice with established human MM, co-administration of Btz and XRK3F2 decreased tumor burden and prevented the progression of MM-induced osteolytic disease by inducing new bone formation more effectively than either single agent alone. The results suggest that p62-ZZ ligands enhance the anti-MM efficacy of proteasome inhibitors and can reduce MM morbidity and mortality by improving bone health.

Introduction

Multiple myeloma (MM) is the second most common hematological malignancy. It affects the elderly and causes skeletal destruction, leading to bone pain and disability.[1,2] First-line therapies rely on several classes of drugs, including proteasome inhibitors (PI) such as bortezomib (Btz), which are the mainstay of MM therapy. However, the development of PI resistance remains a major clinical problem that requires switching to different treatment regimens.[3] Bone complications occur in 80% of MM patients, leading to severe morbidity and increased mortality. Current treatments for MM bone disease are limited to anti-resorptives, which neither inhibit tumor growth nor increase new bone.[1] PI stimulate new bone formation,[4-7] but the effect is transient, allowing the persistence of bone lesions, which often do not heal even during remission.[8] Thus, ways to increase the anti-MM

efficacy of PI are needed to improve therapeutic responses, disease-free survival, and bone health in MM patients.[9]
MM cells secrete abundant monoclonal immunoglobulins, a process requiring assembly of light and heavy chains (HC) during biosynthesis in the endoplasmic reticulum (ER), where HC bind to heat shock protein (HSPA5, also known as GRP78 and BiP) until combined with light chains.[10] HSPA5 cycles out of the ER with proteotoxic cargo (such as excess HC) and is N-terminally, N-Arginine modified.[11] The N-end rule pathway[12] then determines binding to the UBR1 ubiquitin ligase, which targets the cargo to the proteasome for degradation.[13,14] Inhibition of the proteasome induces the alternative second N-end rule pathway by increasing the expression of p62 (SQTSM/sequestosome-1), a multidomain protein scaffold that regulates autophagy, NFκB signaling, necroptosis, and other pathways.[15,16] We previously identified the ZZ-domain of p62 as an important regulator of both

autophagy and signaling pathways in MM and bone cells.[17-19] Ligand binding to the ZZ-domain triggers a conformational switch leading to oligomerization and formation of a liquid phase-separated state that leads to autophagy, RIPK1 binding to the ZZ-domain, which regulates necroptotic cell death,[20] and conformational changes of the ZZ and TBS domains, which affect TRAF6 and NFκB signaling, important regulators of cell survival and bone cell activity.[21-23] We developed a small molecule ligand of the ZZ-domain, XRK3F2, that decreased osteoclast formation and activity[17] and reversed MM-epigenetic suppression of osteoblast differentiation.[18] XRK3F2 as a single agent induced local new bone formation in MM-bearing mice but did not reduce tumor burden.[17]

In this manuscript, we reasoned that XRK3F2 blocks only one of the two branches of the bimodal N-end rule degradation pathway and should be much more effective as an anti-MM agent when combined with a proteasome inhibitor. We report that XRK3F2 amplifies the response to Btz in MM cells by preventing Btz-induced p62 accumulation and triggering simultaneous induction of multiple death pathways. Further, mice with established MM treated with XRK3F2-Btz combination exhibit decreased tumor growth and reduced bone destruction at doses where single agents were ineffective. Collectively, our data show that XRK3F2 boosts both the anti-tumor and bone-anabolic effects of PI and provides a strong rationale for developing a new therapeutic regimen based on co-administration of XRK3F2 and Btz to treat MM.

Methods

Antibodies and compounds
All antibodies and compounds are described in the *Online Supplementary Appendix*.

Human primary CD138+ and bone marrow stromal cell purification and multiple myeloma cell lines
Patient studies were approved by the Indiana University School of Medicine IRB and CD138+ MM cells were isolated as previously described.[24] Human MM cell lines were purchased from ATCC (Manassas, VA, USA) (MM.1S; NCI-H929; RPMI8226) or generously provided by Dr L. Stancato (U266), Dr K. Anderson (KMS-11), and Dr N. Giuliani (JJN3) and cultured in RPMI with 10% fetal calf serum/1% penicillin/streptavidin. Cell line authentication was routinely examined for proper morphology, population doubling, and paraprotein production. HS-5 human stromal cell lines were obtained from ATCC and were cultured in DMEM with 10% fetal calf serum/1% penicillin/streptavidin. All cells were cultured under 37ºC and 5% CO_2 conditions.

Cell viability and apoptosis/necroptosis assays
MM cells were incubated with suboptimal concentrations of XRK3F2 and Btz (below their 24 hour [h] half-maximal inhibitory concentration [IC50]; *Online Supplementary Table S1*) alone or in combination for 24 h ± inhibitors of necroptosis, apoptosis, or autophagy. Cell viability was quantified by alamarBlue® Cell Viability assays from ThermosFisher Scientific (Waltham, MA, USA), according to the manufacturer's protocol. The combined effects of XRK3F2 and Btz on MM cells were evaluated for synergism *versus* additivity by combination index (CI) analysis.[25] A CI less than 1.0 indicates synergism and a CI of 1 indicates additive activity. Lactate dehydrogenase (LDH Cytotoxicity Assay Kit, Thermo Scientific Pierce, 88953) and human high mobility group B (HMGB1, NBP2-62766, Novusbio, Centennial, CO) protein were assayed as markers of necroptosis in cell supernatant and serum, respectively.[26]

Mouse model of human multiple myeloma
Immune-deficient 6-8-week-old Fox Chase SCID (C.B.-17 SCID/SCID) mice Charles River Laboratories (Wilmington, NC) were injected intratibially with $1x10^5$ human JJN3 myeloma cells in 20 μL of phosphate-buffered saline. Mice were handled in accordance with the Guide for the Care and Use of Laboratory Animals, under a protocol approved by the Indiana University School of Medicine IACUC. After 3 weeks mice were treated with either XRK3F2 (27 mg/kg, 5 times per week [5xweek]), Btz (0.25 mg/kg/2xweek), XRK3F2-Btz (27 mg/kg/5xweek plus 0.25 mg/kg/2xweek), or vehicle intraperitoneally (IP) for 2 additional weeks when the mice were euthanized. The sample size was calculated based on a previous study.[17] Details are provided in the *Online Supplementary Appendix*.

Bioinformatic analyses of publicly available datasets
Gene expression data for RIPK3, RIPK1, SQSTM1 (p62), and MLKL were obtained from the MMRF Researcher Gateway using version IA18 and analyzed as described in the *Online Supplementary Appendix*.

Statistical analysis
One- or two-way analysis of variance was performed to determine differences between experimental groups. *Post hoc* comparisons were accomplished via Tukey's and Bonferroni's tests, with statistical significance set *a priori* at $P \leq 0.05$. All statistics were performed using GraphPad Prism 9.3.1, and data are presented as means ± standard deviation. Isobologram analysis was performed using the CalcuSyn software program (Biosoft).

Results

XRK3F2 increases the anti-multiple myeloma efficacy of Btz *in vitro* and *in vivo*
In order to examine whether targeting p62 potentiates the anti-MM effects of PI, we tested the effects of the small molecule ligand of the p62 ZZ-domain, XRK3F2, on MM cell viability as a single agent and in combination with Btz.

Both agents were used at concentrations lower than their IC50 (*Online Supplementary Table S1*). Human MM cells with WT p53 (MM.1S and NCI-H929; Figure 1A; *Online Supplementary Figure 1A*) were more sensitive to Btz than those with mutant p53 (JJN3, RPMI-8226, U266; Figure 1B; *Online Supplementary Figure S1B, C*) or lacking p53 (KMS-11; Figure 1C). Combined treatment significantly reduced MM cell viability compared to either drug alone, independent of p53 status. In order to determine the cause of the decreased MM cell viability, we examined apoptosis in MM1.S cells after 6-hour treatment. Btz alone or combined with XRK3F2 caused significant apoptosis compared to control (*Online Supplementary Figure S1D*). The combination increased the percentage of Annexin V/propidium iodide double-positive cells compared to Btz alone, suggesting increased necrotic cell death. Chou-Talalay analysis showed that XRK3F2-Btz combination had synergistic anti-MM activity against all MM cell lines, with CI values <1. Similar results were obtained in CD138^{+} cells from four relapsed MM patients (Figure 1D). Because the tumor microenvironment (TME) dictates MM cell responses to therapy, we next tested if XRK3F2 overcomes the prosurvival effects of stromal cells on MM cells treated with Btz. Co-culture with stromal cells protected JJN3 MM cells from Btz-induced apoptosis (Figure 1E). In contrast, co-administration of XRK3F2 hampered this protection and resulted in apoptotic levels similar to those in MM cells treated with Btz and cultured alone.

Further, we tested the *in vivo* anti-MM efficacy of single-agent *versus* co-administration of XRK3F2 and Btz in an established xenograft mouse model of human MM (Figure 1F).[27] Three weeks after, JJN3-injected mice, exhibited detectable serum levels of the tumor biomarker human κ light chain, compared to saline-injected mice, indicative of active tumor growth. After 2 weeks, mice bearing MM treated with vehicle exhibited an 8-fold increase in tumor growth. Similar tumor progression was observed in mice receiving single agents. In contrast, the combination therapy reduced tumor burden by 50% compared to vehicle-treated mice and 24% compared to Btz only (Figure 1F; *Online Supplementary Figure S2A*). Dying tumor cells release high-mobility group box 1 protein (HMGB1). Treatment with low doses of XRK3F2 alone or combined with Btz, but not Btz alone, significantly increased serum human HMGB1 (8-fold and 13-fold increase, respectively; *Online Supplementary Figure S2B*). None of the groups lost weight indicating limited toxicity of single agent and combination treatments (*Online Supplementary Figure S2C*). Together, these *in vitro* and *in vivo* results support that XRK3F2-Btz combination decreases tumor growth by activating multiple MM cell death pathways.

XRK3F2 blocks the activation of NFκB and autophagic-survival mechanisms in multiple myeloma cells

Among the multi-domain functions of p62, regulation of NFκB signaling plays a pivotal role in promoting tumor growth and tumor-tumor microenvironment (TME) crosstalk to establish a favorable microenvironment for tumor progression.[28] Additionally, NFκB is the main coordinator of TNF-α signaling, a well-established prosurvival and proliferation factor for MM cells and osteoclasts found in the MM bone marrow microenvironment.[29-31] In MM, Btz increase p62 levels and activate NFκB by downregulating p65-inhibitor IκBα.[32] XRK3F2 treatment prevented NFκB activation triggered by Btz, as shown by a time-dependent reduction in IκBα (*Online Supplementary Figure S3A*). Moreover, XRK3F2 inhibited TNFα-induced IκBα and NFκB[p65] phosphorylation (*Online Supplementary Figure S3B*) and prevented nuclear translocation of NFκB[p65] (*Online Supplementary Figure S3C*) after 5 and 30 minutes respectively, thereby counteracting the prosurvival effects of NFκB activation caused by Btz. These results suggest that XRK3F2 may prevent the NF-κB-dependent protumorigenic effect of Btz, an effect needed especially in relapsed, Btz-resistant MM patients.

Btz increases p62 levels by inducing *de novo* p62 expression and preventing its degradation. In agreement with the previous studies,[33] we found that Btz increased levels of p62 mRNA 8-fold and protein (Figure 2D; *Online Supplementary Figure S2D*) independent of autophagy since changes in LC3I-LC3II conversion were not found in Btz-treated cells. Btz-induced *p62* mRNA expression was reduced by XRK3F2. Ligands binding to p62-ZZ stimulate p62 oligomerization and autophagy.[34] XRK3F2 alone or in combination with Btz increased LC3I-LC3II conversion in MM.1S, indicating induction of autophagy (Figure 2D, left panel). Pretreatment of MM cells with bafilomycin A1 (Baf), which disrupts autophagic flux, further increased LC3II/LC3I ratio and p62 protein levels compared to XRK3F2 alone or XRK3F2-Btz combination (Figure 2D, right panel). Furthermore, autophagy blockade by Baf treatment further amplified the negative effects of XRK3F2 and Btz on MM cell viability (Figure 2A; *Online Supplementary Figure S4A*), indicating that the autophagy-induced by targeting p62-ZZ domain in MM cells was not the pathway responsible for MM cell death.

XRK3F2 and Btz combination treatment activates multiple cell death pathways in multiple myeloma cells

We previously reported that high doses of XRK3F2 triggered caspase 3 cleavage in MM.1S cells.[17] Here, we found that in MM.1S cells, co-administration of 5μM XRK3F2 and 3 nM Btz strongly activated caspase-8 and caspase-3 (Figure 2E, left panel). In contrast, we only detected partial activation of caspases by Btz alone and no activation by XRK3F2 at the concentration used. To test if the increased cell death seen with the combination therapy was due to apoptosis, we used the pan-caspase inhibitor Q-VD-OPh (QVD) and the caspase-3 inhibitor Z-DEVD-FMK (Z-DEV). QVD and Z-DEV completely blocked Btz-induced cleavage of caspase-8 and 3 (Figure 2E, F, right panels). In addition, QVD or Z-DEV fully prevented the decrease in cell viability induced by Btz (Figure 2B, C; *Online Supplementary Figure S4B, C*) but enhanced the anti-MM effects of XRK3F2. QVD and Z-DEV only par-
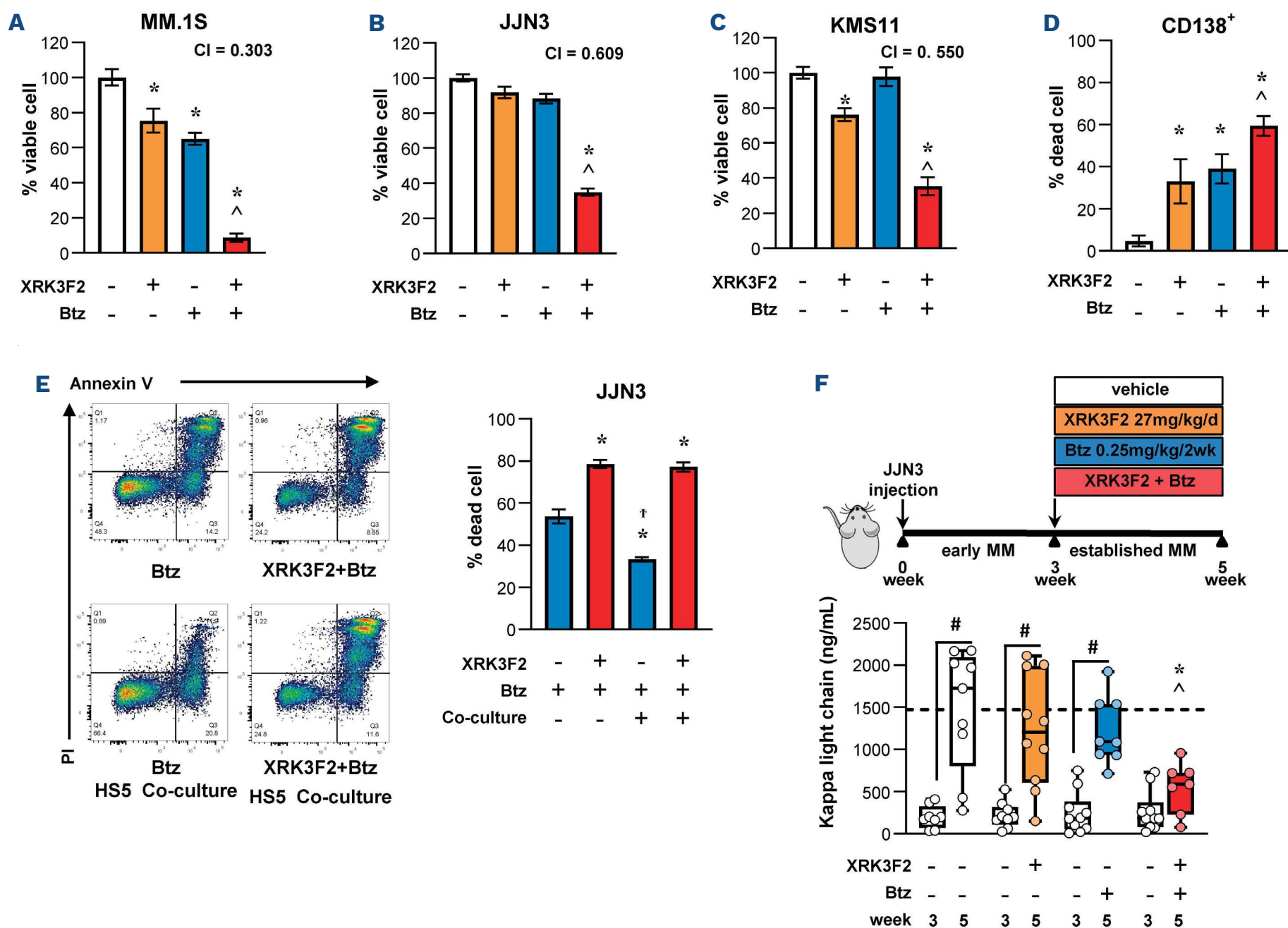
Figure 1. Combination of low doses of XRK3F2 and bortezomib synergistically increases multiple myeloma cell death *in vitro* and inhibits tumor growth *in vivo*. (A) MM.1S; (B) JJN3; (C) KMS-11 and (D) primary CD138+ cells were treated for 24 hours (h) with XRK3F2 (5 μM), bortezomib (Btz) (3 nM), or combined XRK3F2-Btz (5 μM/3 nM). Multiple myeloma (MM) cell viability was evaluated by alamarBlue assay and is reported as percent *versus* dimethyl sulfoxide (DMSO) vehicle control. Combination index (CI) of less than 1 indicates synergy. MM cell death was evaluated by (D) Trypan blue uptake assays or by Annexin V/propidium iodide (PI) staining MM:HS5 cell-to-cell co-cultures after 24 h of treatment (E). Data are presented as bars, means ± standard deviation (N=4-6/group). *$P<0.05$ *versus* vehicle, ^$P<0.05$ *versus* XRK3F2 or Btz alone by one-way ANOVA with *post hoc* Tukey's correction. (F) *In vivo* experimental design (10^5 JJN3 MM cells injected intratibially). Serum levels of the JJN3 tumor biomarker human κ light chain after *in vivo* treatment with XRK3F2 (27 mg/kg/5 times per week [5xweek]), Btz (0.25 mg/kg/2xweek) or XRK3F2-Btz combination. Data are presented as box & whiskers plots where each dot represents a mouse N=7-10/group. #$P<0.05$ *versus* 3 weeks; *$P<0.05$ *versus* JJN3-vehicle and ^$P<0.05$ *versus* JJN3-XRK3F2 or Btz alone by one-way ANOVA with *post hoc* Tukey's correction. The horizontal dotted line indicates the mean value for vehicle-treated mice bearing JJN3 tumors.

tially blocked caspase 8 and 3 cleavage by XRK3F2-Btz and partially reduced the effects of the combination on MM cell viability. These findings suggest that XRK3F2-Btz combination inhibits MM viability by activating both caspase-dependent and independent-cell death pathways.

XRK3F2 increases sensitivity to protease inhibitors by induction of necroptosis

In addition to binding ligand proteins for autophagic degradation, the p62-ZZ domain is also a scaffold for necroptosome formation by binding RIPK1, which forms a complex with RIPK3 and mixed lineage kinase domain-like effector

(MLKL).[20] Inhibition of RIPK1 binding using necrostatin-1 (Nec-1) prevented cell death induced by XRK3F2, but not by Btz, in MM cell lines (Figure 3A; *Online Supplementary Figure S4D*) and CD138+ cells from MM patients (Figure 3B) by preventing the loss of plasma membrane integrity, measured by the LDH release after 16-h culture (Figure 3C). Nec-1 also prevented cell death induced by XRK3F2-Btz combination, inhibiting both necroptosis and RIPK1-dependent apoptosis. Nec-1 did not affect basal autophagy (*Online Supplementary Figure S4E*), suggesting that RIPK1 kinase activity is not required to suppress autophagy. Upon treatment with XRK3F2, RIPK3 co-immunoprecipitated with RIPK1, and
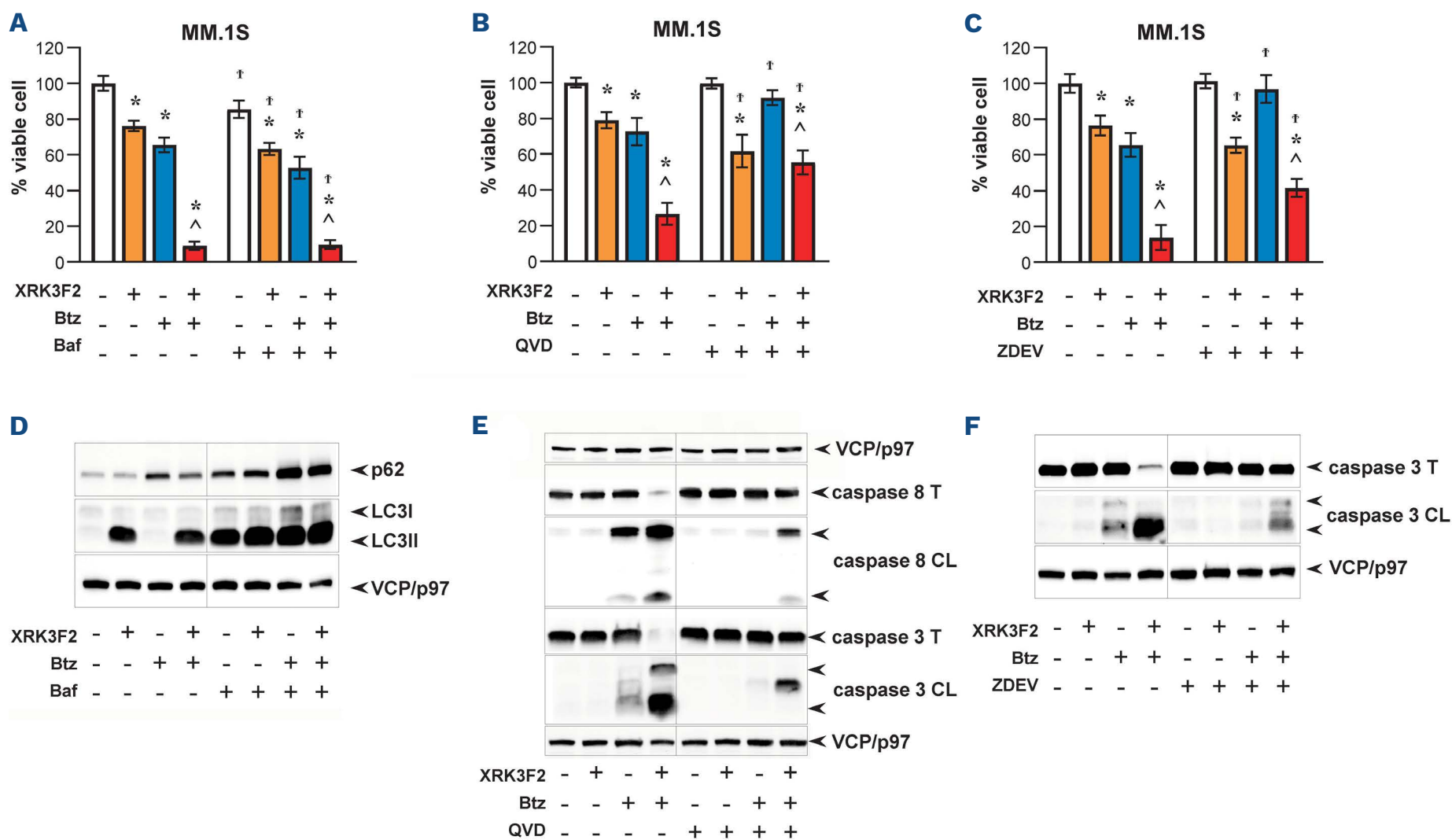
Figure 2. XRK3F2 plus bortezomib combination activates multiple death pathways and overcomes apoptosis resistance in multiple myeloma. MM.1S cells treated with XRK3F2 (5 µM), bortezomib (Btz) (3 nM), or combined XRK3F2-Btz (5 µM/3 nM) for 24 hours in the presence or absence of autophagy inhibitor Bafilomycin A1 (Baf, 40 nM) (A, D), Pan caspase OPH inhibitor Q-VD (QVD, 20 µM) (B, E), or caspase-3 inhibitor Z-DEVD-FMK (Z-DEV, 20 µM) (C, F). Cell viability was evaluated using alamarBlue assays and is reported as percent *versus* dimethyl sulfoxide (DMSO) vehicle control (A-C). Analysis of autophagic flux and apoptosis were assessed by immunoblotting by LC3I-LC3II conversion (D) and for cleavage of caspase 8 and 3 (E, F). Data are presented as bars, means ± standard deviation (N=4-6/group). *$P<0.05$ *versus* vehicle, ^$P<0.05$ *versus* XRK3F2 or Btz alone and ^$P<0.05$ *versus* control *versus* Baf/QVD/ZDEV culture by two-way ANOVA with *post hoc* Bonferroni's correction.

the association was increased by inhibition of apoptosis (Figure 3D, top). XRK3F2-stimulated MLKL phosphorylation at S358 and consequent cell death in MM cells (Figure 3D, bottom). Inhibiting RIPK3 or MLKL phosphorylation with GSK872 (RIPK3 kinase inhibitor) or necrosulfonamide (NSA, an MLKL inhibitor), blocked XRK3F2-induced cell death induced (Figure 3E). Taken together, these results suggest that XRK3F2 treatment leads to induction of necroptosis and synergizes with Btz-mediated apoptosis increasing MM cell death via concurrent activation of multiple death pathways (Figure 3F).

p62 and RIPK3 expression levels inversely correlated with multiple myeloma disease progression

In order to investigate the significance of p62, RIPK1, RIPK3, and MLKL expression in MM patients, publicly available datasets containing normal, monoclonal gammopathy of unknown significance (MGUS), high-risk smoldering MM (SMM), and newly diagnosed MM patients[35] were analyzed. We found that *p62 (SQSTM1)* expression increased at the mRNA level across disease stages with active MM plas-

ma cells (PC) expressing higher p62 levels compared to premalignant MGUS PC (*P*=0.0092; Figure 4A). Further, we observed expression of SQSTM1 in MM cells regardless of International Staging System (ISS) disease stage (*Online Supplementary Figure S5*). RIPK1, RIPK3 and *MLKL* mRNA were all expressed in MM cells albeit *RIPK3* and *MLKL* mRNA levels were significantly reduced in MM patients with active disease compared to MGUS (*P*=0.0206 for *RIPK3*; *P*=0.022 for *MLKL*) and healthy PC (*P*=0.0097 for *RIPK3*; *P*=0.0336 *MLKL*; Figure 4C, D). No significant differences were observed for *RIPK1* (Figure 4B). Further, we confirmed these findings in immunoblots from primary CD138^{+} selected cells from MM patients and MM cell lines (Figure 4E; *Online Supplementary Figure S6*). We observed that p62 was strongly expressed at the protein level in the majority of primary MM cells (10/11 MM patients samples; Figure 4E). RIPK3 and MLKL proteins were detected in 100% (11/11) or 82% (9/11) of the primary CD138^{+} cells from MM patients although their level varied. These data suggest that p62 upregulation and RIPK3/MLKL downregulation correlate with MM disease progression.

Low RIPK3 expression at diagnoses correlates with reduced survival and response to bortezomib-based therapies in multiple myeloma patients

In order to evaluate the impact of the expression of RIPK3, MLKL, and p62 on clinical outcomes for MM patients, we employed the MMRF-CoMMpass (IA18) dataset. Newly diagnosed MM patients (NDMM) with low expression RIPK3 exhibited lower overall survival (OS) (Figure 5A; P=0.00084) and progression-free survival (PFS) (P=0.013) than those with higher expression. We observed similar OS and PFS trends in NDMM patients with low MLKL expression or high p62

expression; however, the results did not reach statistical significance (*Online Supplementary Figure S7A, B*).

Next, we examined if clinical responses to Btz-based therapies correlate with RIPK3 or p62 expression. Among patients receiving Btz-based therapies, those with lower expression of RIPK3 exhibited worse OS (Figure 5B; P=0.00032) and PFS (P=0.017) than those with higher RIPK3 expression. Similar, non-significant trends were observed in Btz-treated patients with low MLKL expression (*Online Supplementary Figure S7C*). In contrast, OS was better in MM patients receiving Btz-based therapy with lower p62 expression (Figure
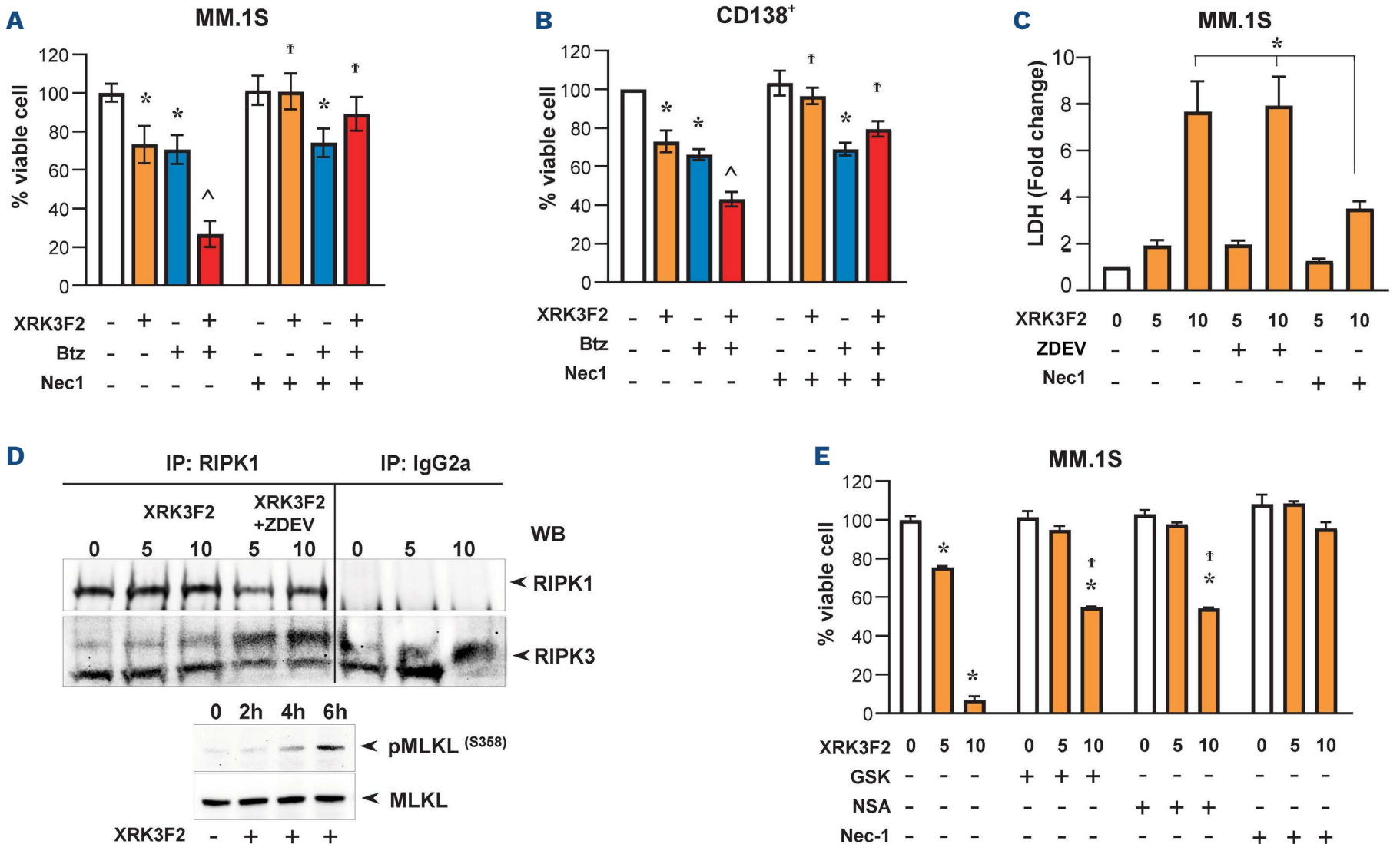

Figure 3. XRK3F2 induces caspase-independent necroptotic cell death. (A) MM.1S and (B) CD138^{+} human multiple myeloma (MM) cells were treated with XRK3F2 (5 μM), bortezomib (Btz) (3 nM), or combined XRK3F2-Btz (5 μM/3 nM) for 24 hours (h) in the presence or absence of RIP1 kinase inhibitor Necrostatin-1 (Nec-1, 60 μM) and viability assayed by alamarBlue assay and is reported as percent *versus* dimethyl sulfoxide (DMSO) vehicle control. (C) MM.1S cells were treated with 0, 5 or 10 μM XRK3F2 for 16 h ± 20 μM Z-DEV or 60 μM Nec-1 followed by lactate dehydrogenase (LDH) release analysis. (D) MM.1S cells were treated with 5 or 10 μM XRK3F2 for 4 h ± 20 μM Z-DEV and RIPK1-RIPK3 binding assessed by immunoprecipitation (IP) using anti-RIPK1 antibody or IgG2a control (top panel). MM.1S cells were treated with 10 μM XRK3F2 for 2, 4, and 6 h, and MLKL phosphorylation at Ser 358 was assessed by western blotting (WB) (bottom panel). (E) MM.1S cells were treated with 0, 5 or 10 μM XRK3F2 for 24 h in the presence or absence of RIP3 kinase inhibitor GSK872 (GSK, 3 μM), MLKL inhibitor necrosulfonamide (NSA, 1 μM) and 60 μM Nec-1. Cell viability was evaluated by alamarBlue and reported as percent *versus* DMSO vehicle control. Data are presented as bars, means ± standard deviation (N=4-6/group). *P<0.05 *versus* vehicle, ^P<0.05 *versus* XRK3F2 or Btz alone, and ⊤P<0.05 control *versus* Nec-1/GSK/NSA culture by two-way ANOVA with *post hoc* Bonferroni's correction. (F) Schematic representation of XRK3F2-Btz combination mechanisms of action.
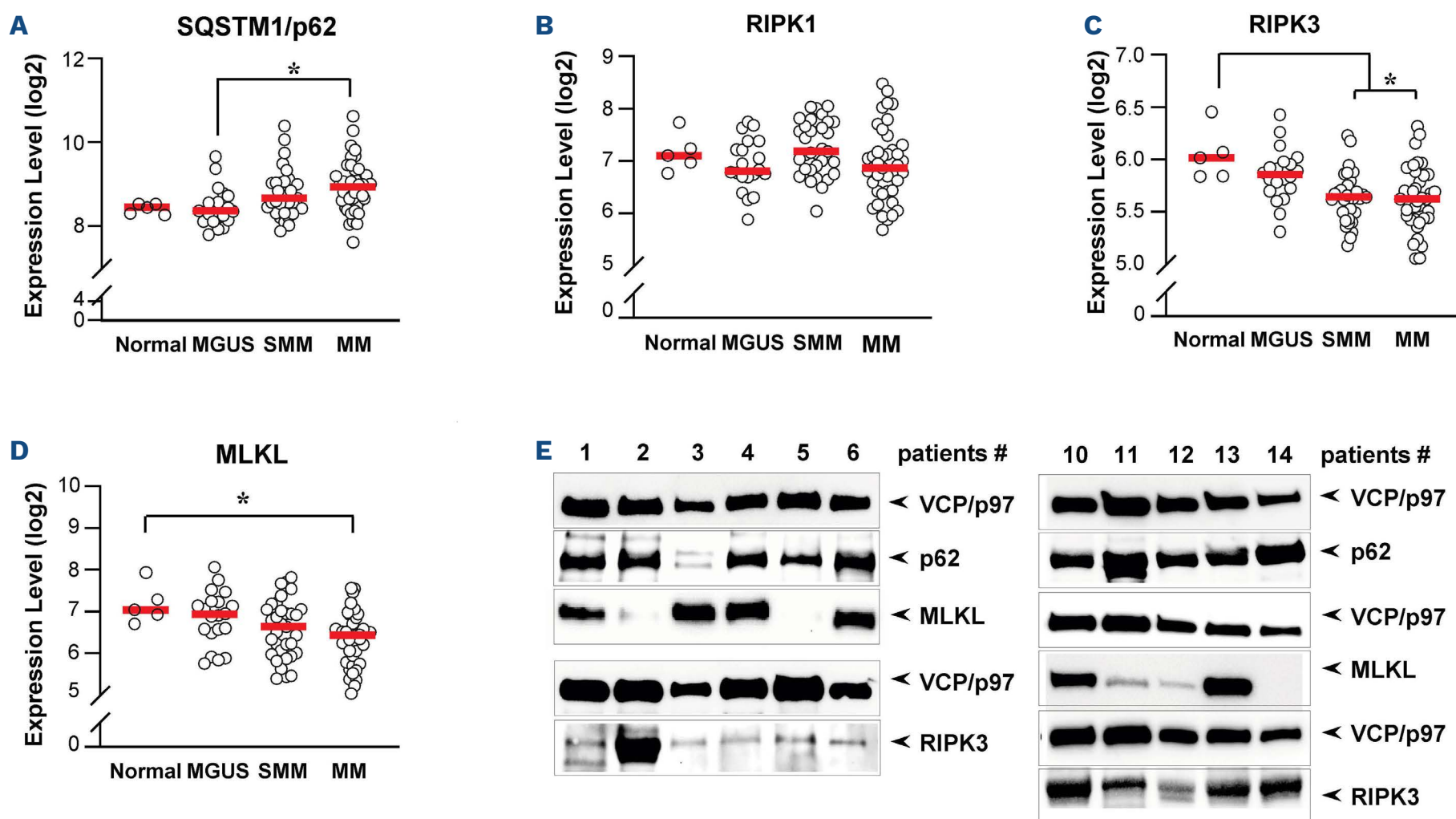
Figure 4. High p62 and low RIPK3 expression in patients correlates with disease progression. Transcriptome analysis of the GDS4968 data set showing the mRNA expression levels in of (A) *p62*, (B) *RIPK1*, (C) *RIPK3* and (D) *MLKL* in CD138^{+} primary cells of multiple myeloma (MM) patients in different stages of the disease monoclonal gammopathy of undetermined significance (MGUS), smoldering MM, or MM and normal plasma cells (N). (E) p62, RIPK3, and MLKL protein expression levels were evaluated by immunoblotting in cell lysates of primary CD138^{+} plasma cells from MM patients ([#]1, 6, 13 newly diagnosed; [#]2 autologous stem cell transplant; [#]3, 5, 10, 14 progressive disease; [#]4, 12 refractory; [#]11 relapsed; *Online Supplementary Table S2*) using VCP/p97 as loading control.

5C; *P*=0.013); although PFS was not affected. Collectively, these results highlight the relevance of the N-rule pathway in clinical responses in MM patients and suggest that modulating RIPK3 and MLKL activities with XRK3F2 can be exploited to improve clinical outcomes in MM patients.

XRK3F2 and Btz combination prevents bone destruction and stimulates bone formation in a human xenograft mouse model of established multiple myeloma disease
MM patients frequently have severe osteolysis leading to increased morbidity and mortality. Whilst PI have been shown to transiently increase bone formation, MM-induced lesions rarely repair. We previously showed that XRK3F2 as a single agent induced cortical bone formation in a syngeneic mouse model of MM.[17] Here, we investigated the effects of XRK3F2 in combination with Btz on an immunodeficient mouse model of human MM bone disease. Three weeks after, JJN3-injected mice showed overt osteolytic lesions in the injected tibias, indicative of established bone disease. No lesions were observed in saline-injected mice. Bone destruction was observed in mice treated with XRK3F2 or Btz alone, while the combination significantly preserved bone mass and reduced the number of osteo-

lytic lesions compared with vehicle or single agent-treated mice (Figure 6A). Both Btz alone and XRK3F2-Btz combination decreased the serum levels of the bone resorption marker CTX compared to vehicle-treated mice. However, only the combination therapy significantly restored serum levels of bone formation marker P1NP to level observed in tumor-naïve mice (Figure 6B). JJN3-injected mice had ~38% decreased cortical bone volume/total volume (BV/TV), measured at the fibular-tibia junction, compared to saline-injected animals. XRK3F2-Btz co-administration mitigated the progression of bone disease by preserving cortical BV/TV (Figure 6C, D). We also performed bone architectural analysis of contralateral tibiae of mice receiving XRK3F2-Btz combination treatment. These bones displayed increased trabecular BV/TV (50%), thickness, Tb.Th (7%), number, Tb.N (45%), and decreased spacing, Tb.Sp (19%), compared to non-MM bearing mice that received vehicle (Figure 7A). Next, we determined the effects of XRK3F2 on osteoblast differentiation and bone-forming activity. Treatment of pre-osteoblastic MC3T3-MC4 cells with XRK3F2-Btz combination increased *Runx2*, *Osterix*, and *Atf4* mRNA expression levels compared to vehicle or single treatment (Figure 7B). The combination, but not the
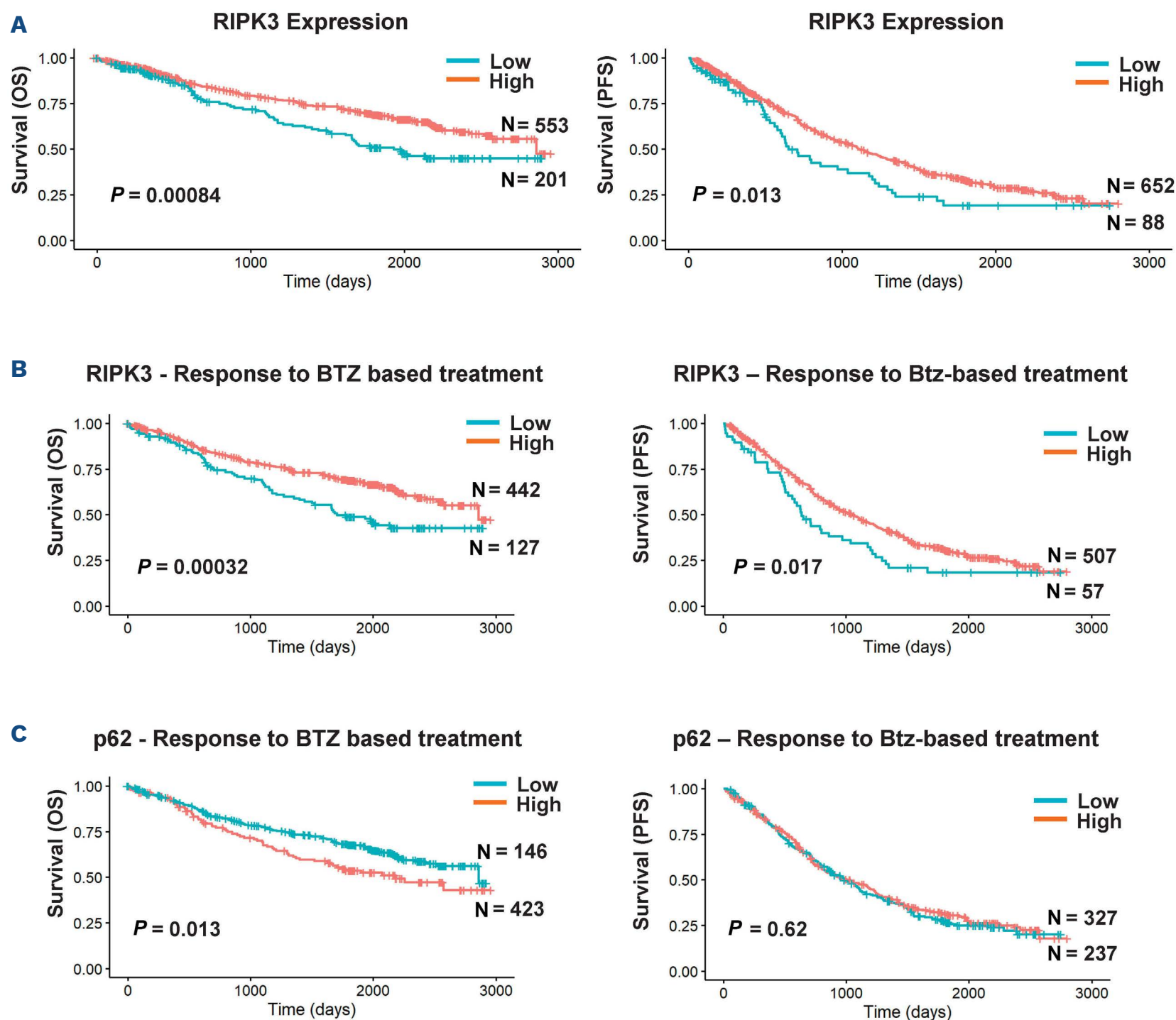
Figure 5. Low RIPK3 correlates with reduced survival and response to bortezomib-based treatment in multiple myeloma patients. Impact of gene expression on overall survival (OS) and progression-free survival (PFS) in patients from the MMRF CoMMpass cohort. (A) OS (left panel) and PFS (days, right panel) in patients with low and high RIPK3 expression. (B) OS (left panel) and OS (days, right panel) in response to bortezomib (Btz)-based therapies in patients with high and low RIPK3 expression. (C) OS (left panel) and PFS (days, right panel) in response to Btz-based therapies in patients with high and low p62 expression.

single agents, also blocked the inhibitory effects of TNFα on osteoblast differentiation by restoring *Runx2* mRNA expression (Figure 7C). XRK3F2-Btz combination but not Btz alone, significantly increased matrix production and mineral deposition of primary bone marrow stromal cells, without affecting viability (Figure 7D). These findings support that XRK3F2 in combination with Btz stimulates bone formation by promoting osteoblast differentiation and activity.

Discussion

MM cells subjected to sustained proteasomal inhibition, as occurs during Btz therapy, rely on p62-mediated autophagic degradation to reduce the proteotoxic load derived from

excessive immunoglobulin (Ig) HC synthesis.[33,36] Excess Ig HC bound to HSPA5 is proteotoxic and induces all three ER stress response regulators: IRE1α, ATF6α, and PERK.[10] HSPA5, with its bound cargo, is exported from the ER to the cytoplasm,[11] where it provides a bimodal degron for cellular elimination.[15] N-Arg bearing substrates are eliminated by either the proteasome following UBR1-catalyzed ubiquitylation or autophagy following binding to the ZZ domain of p62. In the presence of proteasomal inhibition, N-terminally argininylated peptides bind to the p62 ZZ-domain with micromolar affinity and trigger p62 oligomerization[37] and autophagy.[22] Thus, in the presence of PI, p62 provides an alternate pathway for cargo degradation.[15] We developed XRK3F2 by molecular modeling of the ZZ-domain,[17] and Cha-Molstad *et al.*[37] next showed that XRK3F2
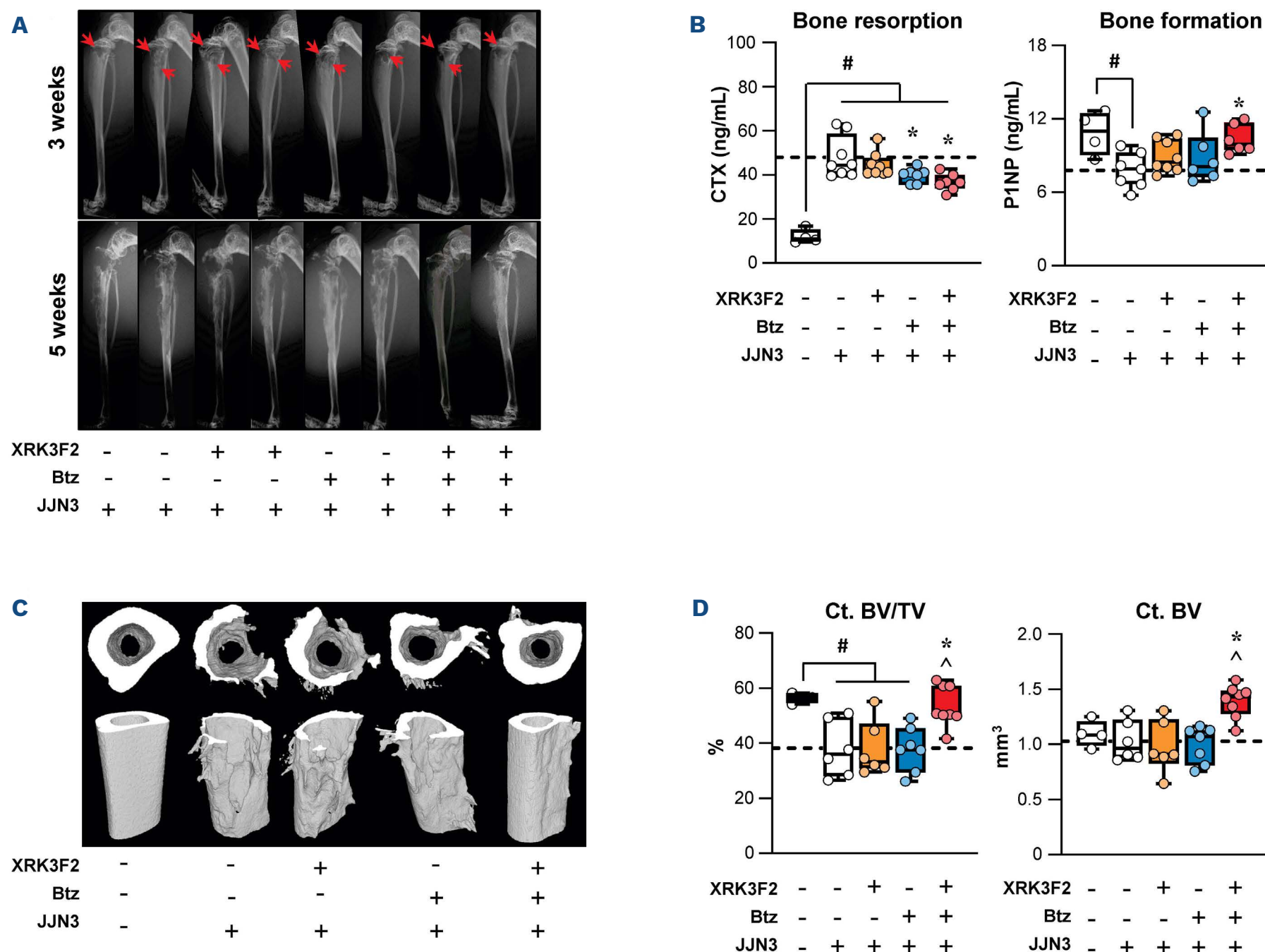
Figure 6. XRK3F2 plus bortezomib combination decreases osteolysis and protects from bone disease progression in mice with established multiple myeloma bone disease. (A) Representative X-rays images of tibiae 3 weeks after JJN3 cell inoculation and 5 weeks after treatment with vehicle (0.01 mL/g in 15% hydroxyl propyl β-cyclodextrin in saline/daily), XRK3F2 (27 mg/kg/5 times per week [5xweek]), bortezomib (Btz) (0.25 mg/kg/2xweek) and XRK3F2-Btz (27 mg/kg/5xweek plus 0.25 mg/kg/2xweek, respectively) for 2 weeks. (B) Bone resorption (CTX, left panel) and bone formation (P1NP, right panel) markers were evaluated by enzyme-linked immunosorbant assay. (C) Representative reconstructed micro-computed tomography (CT) images and (D) analysis of bone microarchitecture of cortical bone of the distal tibia (CT cortical bone volume/tissue volume [BV/TV]; CT BV). Data are presented as box and whiskers plots where each dot represents a mouse N=7-10/group. $^{\#}P<0.05$ *versus* saline-injected mice; $^{*}P<0.05$ *versus* JJN3-vehicle and $^{\wedge}P<0.05$ *versus* JJN3-XRK3F2 or Btz alone by one-way ANOVA. The horizontal dotted line indicates the mean value for vehicle-treated mice bearing JJN3 tumors.

binds to the arginyl-peptide binding site and triggers p62 oligomerization. XRK3F2 functions as a ligand rather than an inhibitor of p62, triggering ineffectual autophagy in the absence of cargo. Thus, the combination of a PI, such as Btz, with XRK3F2 blocks both proteolytic pathways for N-end rule degradation, allowing cytoplasmic accumulation of proteotoxic cargo, such as Ig HCn bound to HSPA5 and subjects MM cells to uncontrolled proteotoxic stress and consequent cell death. Here we demonstrate *in vitro* and *in vivo* that co-administration of suboptimal concentrations of Btz and XRK3F2 synergistically killed MM cells. XRK3F2-Btz combination-induced cell death not only was incompletely prevented by blocking apoptosis or autophagy

but was increased when caspase activation was prevented. These findings are in line with recent evidence showing that apoptosis and necroptosis are tightly connected and can cross-regulate each other.[38] Several recent studies suggested that autophagy is implicated in caspase-independent cell death.[39,40] The significant reduction in cell death induced upon RIP1 kinase inhibition supports necroptosis as a second mechanism of cell death induced by the XRK3F2-Btz combination in both MM cell lines and primary CD138^{+} MM cells. Furthermore, selective pharmacological inhibition of MLKL and RIP3 kinase prevented XRK3F2-induced MM cell death, implying that the viability rescue seen by necroptosis inhibition was not due to off-target effects of
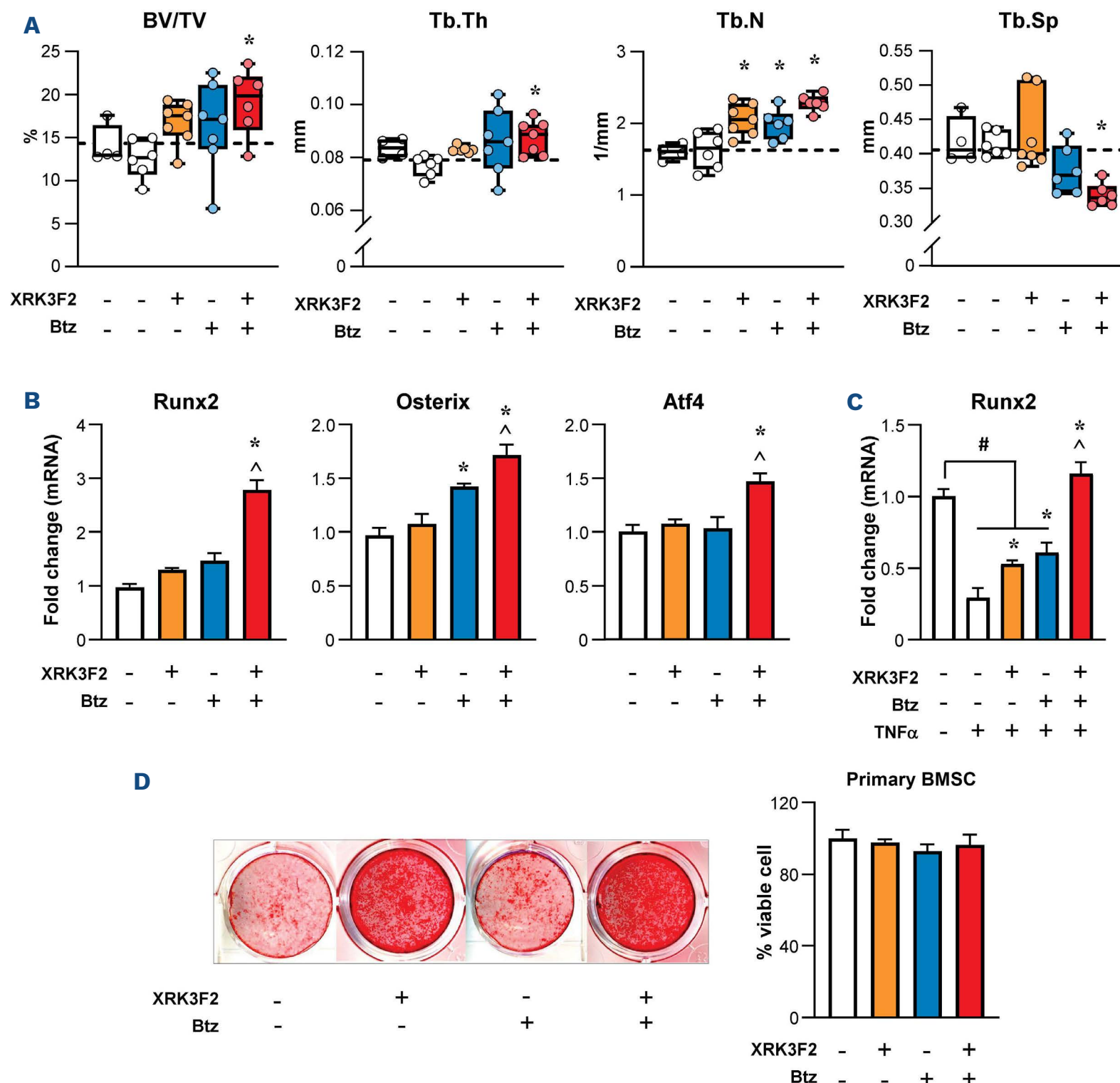
Figure 7. XRK3F2 treatment increases the bone anabolic effects of bortezomib in mice. Analysis of bone microarchitecture of trabecular bone of the contralateral proximal tibia of mice treated with vehicle (0.01 mL/g in 15% hydroxyl propyl β-cyclodextrin in saline/daily), XRK3F2 (27 mg/kg/ 5 times per week [5xweek]); bortezomib (Btz) (0.25 mg/kg/2xweek) and XRK3F2-Btz (27 mg/kg/5xweek plus 0.25 mg/kg/2xweek, respectively) for 2 weeks. (A) Trabecular cortical bone volume/tissue volume (BV/TV), trabecular thickness (Tb.Th), trabecular number (Tb.N), trabecular separation (Tb.Sp). mRNA expression of (B) *Runx2*, *Osterix*, *Atf4* MC3T3-MC4 clones treated for 48 hours (h) with XRK3F2 (100 nM), Btz (2 nM), or combined XRK3F2-Btz (100 nM/2 nM). (C) mRNA expression of *Runx2* in MC3T3-MC4 pre-exposed to 100 ng/mL of TNFα and treated as above and expressed as fold change *versus* vehicle-treated control. (D) Alizarin red staining and viability of primary bone marrow stromal cells (BMSC) cultured treated with XRK3F2 (100 nM), Btz (2nM), or combined XRK3F2/Btz (100 nM/2 nM) for 28 days or 48 h respectively. Data are presented as bars, means ± standard deviation (N=4-6/group). *$P<0.05$ *versus* vehicle, ^$P<0.05$ *versus* XRK3F2 or Btz alone by one-way ANOVA.

Nec1.[41] Several studies have shown that triggering necroptosis in cancer cells can increase chemotherapeutic drug responses (reviewed in[42]). Consistent with the relevant role of this pathway in MM, we found that p62 expression was higher, while RIPK3 and MLKL expression levels were lower, in MM patients compared to MGUS patients, and downregulation of RIPK3 correlated with poor clinical outcomes and responses to Btz-based therapies. These results are consistent with the increase in p62 expression and loss

expression or mutation of components of the necrosome found in other malignancies, and their correlation with poor prognosis.[43,44]

TME plays a central role in MM onset and progression and interactions between MM and cells of the BM transform the marrow into an ideal niche for the migration, proliferation, and survival of MM cells.[45] Adhesion to stromal cells and release of cytokines from them have been shown to decrease the efficacy of chemotherapy on MM

cells by activating prosurvival pathways. We previously showed that XRK3F2 prevented co-culture-induced TNFα upregulation in both 5TGM1 cells and BMSC following co-culture and in BMSC, these effects required p62.[17] Here, although we cannot exclude the contribution of XRK3F2-mediated changes in TNFα production by BM-SC, we show that XRK3F2-Btz combination similarly increased MM cell death regardless of the presence or absence of stromal cells. These results suggest that, in the context of Btz therapy, targeting p62, bypasses the prosurvival and chemoprotective effects of stromal cells for MM cells, making them more susceptible to the pro-apoptotic actions of Btz.

The combination also inhibited the protumoral activation of NFκB and TNFα, crucial factors for the survival and progression of MM and bone cell activity, through additional activities of multiple domains of the p62 scaffold protein.

Most patients with MM suffer skeletal complications characterized by osteolytic bone destruction and inhibited bone formation[1,46] which may persist unhealed during years of remission. Although Btz decreased tumor burden, Btz-treated mice still presented extensive bone lesions. These could be due to the aggressiveness of the mouse model of established bone disease, and/or the suboptimal dose of Btz (0.25 mg/kg/2xweek) used. Nonetheless, even at higher doses, other groups showed that Btz reduces MM burden but was insufficient to reduce osteolytic lesions as a single agent.[9,47] Importantly, while PI can promote transient bone formation, they do not effectively inhibit osteoclasts as single agents.[7]

We previously found that XRK3F2 inhibited osteoclasts, stimulated new bone formation, and increased osteoblast Runx2.[17,18] Here, we found that the combination of XRK3F2 with Btz preserved bone mass in an aggressive mouse model of established human MM bone disease. Further, the combination therapy increased bone mass after only 2 weeks in the contralateral, tumor-free leg. The anabolic action of combination therapy is supported by increased expression of genes associated with mineralization (*Runx2*, *Osterix*, and *Atf4*) and overcoming the suppression of Runx2 by TNFα in osteoblasts.

The detailed mechanism of the positive effects on bone by XRK3F2-Btz remains to be clarified. Activation of ER stress, while killing MM cells, increases osteoblast activity. This activity may involve the XBP1 splicing branch of the tripartite ER stress response, which we have shown is important in both MM and bone cells.[48] XBP1 can affect Btz sensitivity independently of HSPA5, although HSPA5 plays an important role in MM[49] and stimulates osteoblastic mineralization.[50] Our observations are compatible with both HSPA5- and XBP1-dependent mechanisms, which merit further research.

Overall, XRK3F2 provides a multifunctional supplement to proteasome inhibition for treating MM. It synergizes with Btz to kill MM cells by activating necroptosis, while positively suppressing bone destruction with actions on ER stress and proteolytic degradation pathways. XRK3F2 represents a first-in-class ligand for the ZZ-domain of p62, a clinically important multifunctional scaffold protein. XRK3F2 interferes with autophagy and NFκB signaling and activates necroptosis, identifying the ZZ-domain as an important, druggable target for the improved treatment of myeloma bone disease.

Disclosures
No conflicts of interest to disclose.

Contributions
Conceptualization, formal analysis, supervision, investigation, methodology, funding acquisition, writing of original draft, project administration, writing review, and editing by SM. Formal analysis, investigation, methodology, writing review, and editing by DNP. Formal analysis, investigation, methodology writing review, and editing by RTB. Investigation and methodology by JLA, HMS and AC. Investigation, methodology and resources by CA. Formal analysis, investigation and methodology by JHL. Critical manuscript reviewing by UPD. Provision of patient samples by FP. Formal analysis, investigation, methodology, resources, writing review, and editing by J-DC. Conceptualization, supervision, writing of original draft, writing review, and editing by JMC. Conceptualization, resources, supervision, formal analysis, funding acquisition, writing original draft, project administration, writing review, and editing by GDR. All authors read and approved the final manuscript.

Acknowledgments

Funding

Veterans Affairs.

Data-sharing statement
The IA15 datasets used for the analyses described in this work were downloaded from the Multiple Myeloma Research Foundation CoMMpass study (www.themmrf.org) research-

er gateway. The GDS4968 dataset used for the analyses described in this work was downloaded from NCBI's Gene Expression Omnibus (GEO) is a public archive. The datasets used and analyzed to support the conclusions of this article are available from the corresponding author upon reasonable request.

References

1. Marino S, Petrusca DN, Roodman GD. Therapeutic targets in myeloma bone disease. Br J Pharmacol. 2021;178(9):1907-1922.
2. van de Donk N, Pawlyn C, Yong KL. Multiple myeloma. Lancet. 2021;397(10272):410-427.
3. Dima D, Jiang D, Singh DJ, et al. Multiple myeloma therapy: emerging trends and challenges. Cancers (Basel). 2022;14(17):4082.
4. Garrett IR, Chen D, Gutierrez G, et al. Selective inhibitors of the osteoblast proteasome stimulate bone formation in vivo and in vitro. J Clin Invest. 2003;111(11):1771-1782.
5. Oyajobi BO, Garrett IR, Gupta A, et al. Stimulation of new bone formation by the proteasome inhibitor, bortezomib: implications for myeloma bone disease. Br J Haematol. 2007;139(3):434-438.
6. Giuliani N, Morandi F, Tagliaferri S, et al. The proteasome inhibitor bortezomib affects osteoblast differentiation in vitro and in vivo in multiple myeloma patients. Blood. 2007;110(1):334-338.
7. Mukherjee S, Raje N, Schoonmaker JA, et al. Pharmacologic targeting of a stem/progenitor population in vivo is associated with enhanced bone regeneration in mice. J Clin Invest. 2008;118(2):491-504.
8. Marino S, Roodman GD. Multiple myeloma and bone: the fatal interaction. Cold Spring Harb Perspect Med. 2018;8(8):a031286.
9. Tao J, Srinivasan V, Yi X, et al. Bone-targeted bortezomib inhibits bortezomib-resistant multiple myeloma in mice by providing higher levels of bortezomib in bone. J Bone Miner Res. 2022;37(4):629-642.
10. van Anken E, Bakunts A, Hu CA, Janssens S, Sitia R. Molecular evaluation of endoplasmic reticulum homeostasis meets humoral immunity. Trends Cell Biol. 2021;31(7):529-541.
11. Shim SM, Choi HR, Sung KW, et al. The endoplasmic reticulum-residing chaperone BiP is short-lived and metabolized through N-terminal arginylation. Sci Signal. 2018;11(511):eaan0630.
12. Varshavsky A. The N-end rule pathway and regulation by proteolysis. Protein Sci. 2011;20(8):1298-1345.
13. Cha-Molstad H, Sung KS, Hwang J, et al. Amino-terminal arginylation targets endoplasmic reticulum chaperone BiP for autophagy through p62 binding. Nat Cell Biol. 2015;17(7):917-929.
14. Kwon DH, Park OH, Kim L, et al. Insights into degradation mechanism of N-end rule substrates by p62/SQSTM1 autophagy adapter. Nat Commun. 2018;9(1):3291.
15. Yoo YD, Mun SR, Ji CH, et al. N-terminal arginylation generates a bimodal degron that modulates autophagic proteolysis. Proc Natl Acad Sci U S A. 2018;115(12):E2716-e2724.
16. Kumar AV, Mills J, Lapierre LR. Selective autophagy receptor p62/SQSTM1, a pivotal player in stress and aging. Front Cell Dev Biol. 2022;10:793328.
17. Teramachi J, Silbermann R, Yang P, et al. Blocking the ZZ domain of sequestosome1/p62 suppresses myeloma growth and osteoclast formation in vitro and induces dramatic bone formation in myeloma-bearing bones in vivo. Leukemia. 2016;30(2):390-398.
18. Adamik J, Silbermann R, Marino S, et al. XRK3F2 inhibition of p62-ZZ domain signaling rescues myeloma-induced GFI1-driven epigenetic repression of the Runx2 gene in pre-osteoblasts to overcome differentiation suppression. Front Endocrinol (Lausanne). 2018;9:344.
19. Hiruma Y, Honjo T, Jelinek DF, et al. Increased signaling through p62 in the marrow microenvironment increases myeloma cell growth and osteoclast formation. Blood. 2009;113(20):4894-4902.
20. Goodall ML, Fitzwalter BE, Zahedi S, et al. The autophagy machinery controls cell death switching between apoptosis and necroptosis. Dev Cell. 2016;37(4):337-349.
21. Hennig P, Fenini G, Di Filippo M, Karakaya T, Beer HD. The pathways underlying the multiple roles of p62 in inflammation and cancer. Biomedicines. 2021;9(7):707.
22. Komatsu M. p62 bodies: Phase separation, NRF2 activation, and selective autophagic degradation. IUBMB Life. 2022;74(12):1200-1208.
23. Marino S, Bishop RT, Logan JG, Mollat P, Idris AI. Pharmacological evidence for the bone-autonomous contribution of the NFκB/β-catenin axis to breast cancer related osteolysis. Cancer Lett. 2017;410:180-190.
24. Petrusca DN, Mulcrone PL, Macar DA, et al. GFI1-dependent repression of SGPP1 increases multiple myeloma cell survival. Cancers (Basel). 2022;14(3):772.
25. Chou TC. Drug combination studies and their synergy quantification using the Chou-Talalay method. Cancer Res. 2010;70(2):440-446.
26. Shlomovitz I, Zargarian S, Erlich Z, Edry-Botzer L, Gerlic M. Distinguishing necroptosis from apoptosis. Methods Mol Biol. 2018;1857:35-51.
27. Sabol HM, Ferrari AJ, Adhikari M, et al. Targeting notch inhibitors to the myeloma bone marrow niche decreases tumor growth and bone destruction without gut toxicity. Cancer Res. 2021;81(19):5102-5114.
28. Moscat J, Diaz-Meco MT. p62 at the crossroads of autophagy, apoptosis, and cancer. Cell. 2009;137(6):1001-1004.
29. Jourdan M, Tarte K, Legouffe E, et al. Tumor necrosis factor is a survival and proliferation factor for human myeloma cells. Eur Cytokine Netw. 1999;10(1):65-70.
30. Hayden MS, Ghosh S. Regulation of NF-κB by TNF family cytokines. Semin Immunol. 2014;26(3):253-266.
31. Novack DV. Role of NF-κB in the skeleton. Cell Res. 2011;21(1):169-182.
32. Hideshima T, Ikeda H, Chauhan D, et al. Bortezomib induces canonical nuclear factor-kappaB activation in multiple myeloma cells. Blood. 2009;114(5):1046-1052.
33. Milan E, Perini T, Resnati M, et al. A plastic SQSTM1/p62-

dependent autophagic reserve maintains proteostasis and determines proteasome inhibitor susceptibility in multiple myeloma cells. Autophagy. 2015;11(7):1161-1178.

34. Zhang Y, Mun SR, Linares JF, et al. ZZ-dependent regulation of p62/SQSTM1 in autophagy. Nat Commun. 2018;9(1):4373.

35. Lopez-Corral L, Corchete LA, Sarasquete ME, et al. Transcriptome analysis reveals molecular profiles associated with evolving steps of monoclonal gammopathies. Haematologica. 2014;99(8):1365-1372.

36. Sha Z, Schnell HM, Ruoff K, Goldberg A. Rapid induction of p62 and GABARAPL1 upon proteasome inhibition promotes survival before autophagy activation. J Cell Biol. 2018;217(5):1757-1776.

37. Cha-Molstad H, Yu JE, Feng Z, et al. p62/SQSTM1/ Sequestosome-1 is an N-recognin of the N-end rule pathway which modulates autophagosome biogenesis. Nat Commun. 2017;8(1):102.

38. Bertheloot D, Latz E, Franklin BS. Necroptosis, pyroptosis and apoptosis: an intricate game of cell death. Cell Mol Immunol. 2021;18(5):1106-1121.

39. Goodall ML, Cramer SD, Thorburn A. Autophagy complexes cell death by necroptosis. Oncotarget. 2016;7(32):50818-50819.

40. Feldmann F, Schenk B, Martens S, Vandenabeele P, Fulda S. Sorafenib inhibits therapeutic induction of necroptosis in acute leukemia cells. Oncotarget. 2017;8(40):68208-68220.

41. Cho Y, McQuade T, Zhang H, Zhang J, Chan FK. RIP1-dependent and independent effects of necrostatin-1 in necrosis and T cell activation. PLoS One. 2011;6(8):e23209.

42. Gong Y, Fan Z, Luo G, et al. The role of necroptosis in cancer biology and therapy. Mol Cancer. 2019;18(1):100.

43. Sánchez-Martín P, Saito T, Komatsu M. p62/SQSTM1: 'Jack of all trades' in health and cancer. FEBS J. 2019;286(1):8-23.

44. Najafov A, Chen H, Yuan J. Necroptosis and cancer. Trends Cancer. 2017;3(4):294-301.

45. Neumeister P, Schulz E, Pansy K, Szmyra M, Deutsch AJ. Targeting the microenvironment for treating multiple myeloma. Int J Mol Sci. 2022;23(14):7627.

46. Bernstein ZS, Kim EB, Raje N. Bone disease in multiple myeloma: biologic and clinical implications. Cells. 2022;11(15):2308.

47. Wallington-Beddoe CT, Bennett MK, Vandyke K, et al. Sphingosine kinase 2 inhibition synergises with bortezomib to target myeloma by enhancing endoplasmic reticulum stress. Oncotarget. 2017;8(27):43602-43616.

48. Xu G, Liu K, Anderson J, et al. Expression of XBP1s in bone marrow stromal cells is critical for myeloma cell growth and osteoclast formation. Blood. 2012;119(18):4205-4214.

49. Ninkovic S, Harrison SJ, Quach H. Glucose-regulated protein 78 (GRP78) as a potential novel biomarker and therapeutic target in multiple myeloma. Expert Rev Hematol. 2020;13(11):1201-1210.

50. Ravindran S, Gao Q, Ramachandran A, et al. Stress chaperone GRP-78 functions in mineralized matrix formation. J Biol Chem. 2011;286(11):8729-8739.